Published in final edited form as:
Calcif Tissue Int. 2007 September ; 81(3): 206–214. doi:10.1007/s00223-007-9045-x.

Abnormal Mineral-Matrix Interactions Are a Significant Contributor to Fragility in *oim/oim* Bone

Elizabeth Miller,
Musculoskeletal Integrity Program, Research Division, Hospital for Special Surgery, 535 E. 70th Street, New York, NY 10021, USA

Demetris Delos,
Musculoskeletal Integrity Program, Research Division, Hospital for Special Surgery, 535 E. 70th Street, New York, NY 10021, USA

Todd Baldini, **Timothy M. Wright**, and
Musculoskeletal Integrity Program, Research Division, Hospital for Special Surgery, 535 E. 70th Street, New York, NY 10021, USA

Nancy Pleshko Camacho
Musculoskeletal Integrity Program, Research Division, Hospital for Special Surgery, 535 E. 70th Street, New York, NY 10021, USA

Nancy Pleshko Camacho: camachon@hss.edu

Abstract

The presence of abnormal type I collagen underlies the tissue fragility in the heritable disease osteogenesis imperfecta (OI), though the specific mechanism remains ill-defined. The current study addressed the question of how an abnormal collagen-based matrix contributes to reduced bone strength in OI by comparing the material properties of mineralized and demineralized bone from the *oim/oim* mouse, a model of OI that contains homotrimeric ($\alpha 1_3$(I)) type I collagen, with the properties of bone from wildtype (+/+) mice. Femoral three-point bend tests combined with geometric analyses were conducted on intact (mineralized) 14-week-old *oim/oim* and +/+ mice. To investigate the bone matrix properties, tensile tests combined with geometric analyses were conducted on demineralized femora. The majority of the properties of the mineralized *oim/oim* bone were inferior to those of the +/+ bone, including greater brittleness (+78.6%) and lower toughness (−69.2%). In contrast, tensile measurements on the demineralized bone revealed no significant differences between the *oim/oim* and +/+ bone, indicating that the matrix itself was not brittle. These results support the concept that deficient material properties of the demineralized bone matrix itself are not the principal cause of the severe fragility in this model of OI. It is likely the abnormal collagen scaffold serves as a template for abnormal mineral deposition, resulting in an incompetent mineral-matrix interaction that contributes significantly to the inferior material properties of bone in *oim/oim* mice.

Keywords

Biomechanics; Bone; Collagen; Mice; Mineral; Osteogenesis imperfecta

Correspondence to: Nancy Pleshko Camacho, camachon@hss.edu.

Present Address: E. Miller, New York University School of Medicine, 530 First Avenue, New York, NY 10016, USA
Present Address: T. Baldini, UCHSC @ Fitzsimons, 13001 E. 17th Place, Bldg. 500, Rm. NG005, Aurora, CO 80010, USA

Osteogenesis imperfecta Osteogenesis imperfecta (OI) is a heritable disease of the connective tissues characterized by tissue fragility and skeletal deformities. The molecular basis for most forms of this heterogeneous disease lies in mutations of the genes that encode for type I procollagen [1]. These mutations lead to abnormal α1 or α2 chains that may not assemble correctly into the normal collagen fibril, resulting in changes in fibril size, orientation, packing, and crosslinking [2–7]. The bone fragility characteristic of OI is attributed to this abnormal collagen production, but the underlying mechanism linking the abnormality to the fragility remains ill defined. It is unclear whether the abnormal collagen alters mechanical properties of OI bone via a primary effect, whereby the mutant collagen itself is less competent than normal collagen, or alternatively whether the abnormal scaffold may "direct" abnormal mineral deposition that in turn results in reduced mechanical competence of the collagen-mineral composite and increased fragility.

There is evidence to support the notion that disrupted extracellular matrix in OI patients serves as an abnormal template for mineral deposition, leading to altered bone density [8–10], as well as mineral crystals of abnormal shape, size, composition, and alignment [8,11–14]. However, there have been no studies directly examining the mechanical or material properties of the collagen of OI patients. To address the effect of an abnormal matrix phase on bone properties, we utilized the *oim/oim* mouse, a model of OI that is deficient in proα2(I) collagen. Mice homozygous for the *oim* mutation exhibit a moderate-to-severe OI phenotype characterized by skeletal fractures and deformities, osteopenia, and small body size [15]. The *oim/oim* bone has a mineral phase with chemical composition abnormalities [16], a higher mineral:matrix (mineral tissue density), a lower carbonate content, and a less crystalline structure [17–19]. In addition, several studies have demonstrated reduced mechanical properties of the long bones of *oim/oim* mice at both the structural and material level [17,20–22], including increased brittleness, reduced stiffness, and the ability to withstand significantly less load to failure compared with +/+ bone.

To investigate the source of bone fragility at the material level in *oim/oim* mice, we assessed the properties of the matrix phase of *oim/oim* femora. This was accomplished by evaluating the tensile characteristics of demineralized *oim/oim* femora and comparing these with the material properties of mineralized bone determined from three-point bending tests combined with geometrical analyses. The results of these experiments provide a direct answer to the question of whether the *oim/oim* bone matrix is itself "brittle" or whether the brittleness and mechanical incompetence of these bones arise from the abnormal mineral-matrix interaction.

Materials and Methods

Animals

All animal procedures were performed under an IACUC-approved protocol. To obtain the *oim/oim* mice, heterozygous *oim* breeder mice (*oim*/+) were purchased from the Jackson Laboratory (Bar Harbor, ME). Average litter sizes were 8–12 pups of which approximately 25% were *oim/oim*. However, the survival rate of the homozygous *oim* pups was often less than 50%; thus, to augment the number of pups for the study, male *oim/oim* mice were bred to female *oim*/+. In addition, wildtype (+/+) breeder pairs were utilized to obtain the +/+ mice needed for the control group. All mice received Purina rodent chow and tap water *ad libitum* and were kept at 24°C.

Upon weaning of the pups at approximately 4 weeks of age, tail snips 1 cm long were obtained for genotype determination [23]. A total of 58 femora from 48 mice were tested either in a three-point bend test or in tension. Fourteen +/+ and 15 *oim/oim* femora were utilized for three-point bend tests, and 17 +/+ and 12 *oim/oim* femora were utilized for tensile tests, with approximately equal numbers of males and females in each group. We were unable to perform

paired tests, i.e., utilizing one femur from each mouse for a three-point bend test and one femur for a demineralized tensile test, due to the high fracture rate of the *oim/oim* femora. At 14 weeks of age, mice were killed by carbon dioxide inhalation. The right and left femora from each animal were harvested, and the bones, devoid of soft tissue, were wrapped in gauze soaked in pH 7.4 Tris buffer and kept frozen at −20°C until use.

Geometrical Analysis

Faxitron radiographs (Hewlett Packard, Rockville, MD, USA) were obtained in the anterior-posterior (AP) and medial-lateral (ML) planes. Femoral length was determined as the distance from the tip of the femoral head to the base of the condyles. Endosteal (d_e) and periosteal (d_p) diameters in the AP and ML planes were measured at the femoral midpoint from digitized radiographs (resolution 1524 × 1012 pixels) using Sigma Scan software (Jandel Scientific, San Rafael, CA, USA). Based on the diameter measurements, the femoral cross-section was estimated to be elliptical. The moment of inertia, *I*, was calculated as:

$$I_{\text{ellipse}} = \frac{\pi}{4}\left[\left(\frac{APd_p}{2}\right)\left(\frac{MLd_p}{2}\right)^3 - \left(\frac{APd_e}{2}\right)\left(\frac{MLd_e}{2}\right)^3\right]$$

where APd_p in the AP plane view corresponds to the major periosteal diameter of the ellipse, MLd_p in the ML plane view corresponds to the minor periosteal diameter, APd_e in the AP plane view corresponds to the major endosteal diameter of the ellipse, and MLd_e in the ML plane view corresponds to the minor endosteal diameter. This estimate of femoral moment of inertia is frequently used [24] and correlates significantly with microCT assessment of moment of inertia [25]. The cross-sectional area, *A*, was calculated as:

$$A_{ellipse} = (\pi)\left[(APd\text{p})(MLd\text{p}) - (APd\text{e})(MLd\text{e})\right]$$

Mineralized Bones: Three-Point Bend Tests

Three-point bend tests were performed as previously described [22]. One femur from each mouse was utilized for mechanical testing. For the *oim/oim* mice, the femur chosen for testing was confirmed to contain no fractures or deformations. Three-point bend tests were conducted at room temperature using a closed-loop servo-hydraulic uniaxial MTS test frame (MTS Systems, Eden Prairie, MN, USA) with Instron electronic controls (Instron, Canton, MA, USA). The anterior surface of the femur was placed on the load supports, and the load was applied posteriorly at the mid-diaphysis. For this configuration, the posterior surface is in compression and the anterior surface experiences tension. Since there was less than a 3% difference in average bone length among specimens (15.25 ± 0.38 vs 15.60 ± 0.19 for the *oim/oim* versus +/+ femora, respectively), a set distance of 8 mm was used for the outside loading points. The tests were performed at a rate of 0.5 N/sec, and load and displacement data were acquired at 20 Hz with a PC equipped with a 12 bit A/D data acquisition board. Specimens were kept wet throughout testing.

Both structural (whole bone) properties and intrinsic material (tissue) properties of the bone were calculated using accepted formulas for bone testing [24,26]. For structural properties, ultimate load was defined as the maximum load the bone sustained during testing, and deflection was assumed to be equal to the amount of crosshead deflection during testing. Stiffness was calculated as the slope of the linear region of the load-deflection curve, and work was calculated as the area under the load-deflection curve. For material properties, the stress was calculated as:

$$\sigma = \frac{Mc}{I_{ellipse}}$$

where M is the moment, c is the distance from the neutral axis to the most anterior point on the bone cross-section (equal to ½ APd_p when approximating the cross-section to be elliptical), and $I_{ellipse}$ is the moment of inertia. Strain was calculated as:

$$\varepsilon = \frac{12cd}{L^2}$$

where c is the medial-lateral outside radius (½ MLd_p), d is the crosshead displacement, and L is the span between the loading supports. Elastic modulus (the slope of the linear elastic region of the curve, a measure of the intrinsic stiffness of the material) and ultimate stress (the maximum stress before failure) were determined from the resulting stress-strain curves. Toughness (a measure of the amount of energy needed to fracture the bone tissue) was calculated as the area under the stress-strain curve. Materials that sustain very little post-yield strain before fracture are termed “brittle”, and thus the “brittleness” of the cortical bone, a material property, was calculated by dividing the yield strain (point of maximum elastic deformation) by the ultimate strain.

Demineralized Bones: Demineralization and Embedding

A pilot study was performed on three +/+ and three *oim/oim* femora to determine the minimum time needed for complete demineralization. A 0.5 M solution of ethylen-ediaminetetraacetic acid (EDTA, tetrasodium salt) buffered to a pH of 7.4 at 4°C was utilized. Each femur was immersed in 15 ml of EDTA and left on a shaker at 4°C for a total of 7 days [27]. The EDTA solution was replaced daily to expedite demineralization and prevent significant pH changes in the solution. To determine the quantity of calcium extracted each day, an aliquot of the EDTA solution was analyzed by atomic absorption spectrophotometry [28]. After 48 hr, no further extraction of Ca^{2+} took place (data not shown). Radiographs of the demineralized samples confirmed the absence of the mineral phase.

The EDTA aliquots were also analyzed for protein content to ensure that the demineralization process did not draw a significant amount of non-collagenous proteins into solution. To isolate the proteins from smaller molecules, the aliquots were passed through prepacked 11.5 cm × 5 cm Sephadex G-25 columns (Pharmacia). The protein content of the eluent fractions was assessed using the Bio-Rad protein microassay [29]. This assay is reproducible with little or no interference from cations and carbohydrates [30]. All EDTA aliquots displayed a protein concentration far below the low end of the linear range of the protein microassay (8 μg/ml), which represents less than 3% of the total estimated non-collagenous proteins present.

Following the pilot study and prior to demineralization, the ends of the *oim/oim* and +/+ femora were embedded in PMMA denture acrylic resin. This technique allows for the demineralization of the diaphysis of the bone, while leaving the metaphysis and epiphysis intact [27]. During embedding, the femora were supported and guided in the potting apparatus using a custom-machined Plexiglas insert to help ensure axial alignment. Once the PMMA had cured, femora were demineralized in EDTA at 4°C for 48 hr. The EDTA solution was changed after the first 24 hr. Complete demineralization of the test specimens was confirmed radiographically.

Demineralized Bones: Tensile Testing

Tensile testing was conducted at room temperature using the same servohydraulic test system as for the bend tests. The embedded ends of the demineralized femora were mounted onto one grip fixed to the actuator of the test frame and another grip connected to a 250 N load cell fixed to the crosshead of the test system (Fig. 1). A universal joint was included in the load train to ensure that the specimens experienced pure axial loading. Each femur was loaded to failure under displacement control at a rate of 0.01 mm/sec. All demineralized femora fractured at failure, and this was considered to be the endpoint of the test. Load data were acquired at 5 Hz into the same PC as was used for the bend tests. Samples were kept wet throughout testing. Displacement data were obtained using a digital camera tracking system (Qualysis, Glastonburg, CT, USA). Small reflective markers (3M) were placed on the surface of the embedded ends of the femora. The movements of these markers were recorded in pixel coordinates at 5 Hz, and the resolution of the measurement of the digital camera tracking system was better than 50 μm. The reflective markers ensured that the measured displacements were occurring in the bone tissue itself and not outside the gripped area and within the testing machine.

Stress, σ, was calculated from load data as follows:

$$\sigma = F / A_{ellipse}$$

where F is the force (or load), and $A_{ellipse}$ is the cross-sectional area of the femur at its midpoint. The midpoint value was utilized because the failure pattern of the demineralized bone did not allow for a cross-sectional area at the exact point of failure to be determined after testing. The pixel coordinates captured by the digital tracking system were converted to strain using:

$$\varepsilon = \Delta l / l_o$$

where Δl and l_o are the change in length and the original length (in pixel coordinates) between the markers, respectively. As deflection values (i.e., in millimeters) were not measured, the structural properties of stiffness and work were not calculated.

From the resulting stress-strain curves, the elastic modulus was determined as the slope of the elastic region of the curve between 20% and 80% of the maximum stress (MPa). Since a yield region did not occur, brittleness was not calculated as in the mineralized tissues. Instead, comparison of maximum strain between the two genotypes was utilized as an indicator of brittleness. Maximum stress and strain were determined as the values at failure. Toughness was calculated as the area under the stress-strain curve until the point of failure.

Demineralized Bones: Fracture Surface

The fracture surfaces of the tensile-tested demineralized bones were qualitatively evaluated for fracture pattern. The femora were evaluated under a dissecting microscope and the fracture patterns described as either oblique, when the line of fracture was at an approximately 45° angle to the long axis of the bone, or transverse, when the line of fracture was approximately perpendicular to the long axis of the bone.

Statistical Analysis

Statistical analyses were performed with SigmaStat software (SPSS, Chicago, IL, USA). Means and standard deviations were calculated for each measured parameter. Comparisons

were made between the two groups using the Student's *t*-test to determine the probability of differences. Values were considered significantly different at $p < 0.05$.

Results

Mineralized Bones: Three-Point Bend Tests

Although this work focuses primarily on material properties, here we also present structural properties of the mineralized bone for comparison. As previously reported [22], all the structural and material properties of the *oim/oim* bone were inferior to those of the +/+ bone, with the exception of elastic modulus, which was greater (Tables 1, 2). Ultimate stress was 14% lower, ultimate strain and toughness were more than 50% lower compared with the +/+ values, and brittleness was almost doubled. This was attributed to the virtual absence of plastic deformation in the *oim/oim* tissues.

Tensile Testing

All demineralized bone specimens subjected to tensile loading were completely flexible. For both groups, the mechanical tests generally produced stress-strain curves that exhibited initial nonlinear "toe" and "heel" regions, followed by a linear region (Fig. 2). Failure occurred without yielding in nearly all the samples tested. The +/+ demineralized bones failed very obliquely in a consistent manner, while the *oim/oim* demineralized bones failed in various patterns, including oblique and transverse. The mean *oim/oim* value for ultimate stress was approximately 25% lower than that of the +/+, but did not reach significance ($p = 0.09$; Table 3). There were also no significant differences in the mean values for ultimate strain, elastic modulus or toughness between the two genotypes.

Comparison of Material Properties of Mineralized and Demineralized Bone

The primary difference between the material properties of the mineralized and demineralized *oim/oim* and +/+ bones lies in the relative values of ultimate strain (Fig. 3). For the mineralized bone, there was a striking reduction of approximately 59% in the ultimate strain of the *oim/oim* compared with the +/+ bone, which resulted in a significantly more brittle tissue. However, once the mineral was removed, the ultimate strains of the +/+ bone matrix and the *oim/oim* bone matrix were essentially equivalent. The fact that the ultimate strain of the *oim/oim* demineralized bone was nearly normal also contributed to the toughness of the demineralized bone being only 25% less compared to that of the +/+ bone, an amount equivalent to the reduction in ultimate stress. In addition, the elastic modulus of the demineralized bone was nearly equivalent for the two genotypes. This is in sharp contrast to the finding for the mineralized bone, where the elastic modulus was approximately 44% greater for the *oim/oim* bones, attributable to the very small strain to failure for the femora of these mice.

Discussion

The present study addressed the mechanism by which an abnormal collagen matrix contributes to reduced bone strength in OI by comparing the material properties of mineralized and demineralized *oim/oim* and +/+ mouse bone. We found that the differences between the material properties of the demineralized *oim/oim* and +/+ demineralized bone matrices were substantially less than the differences between the properties of the mineralized bone for these two genotypes. Furthermore, the largest difference in any demineralized bone matrix property was the nonsignificant 25% reduction in ultimate stress of the *oim/oim* mice compared with the +/+ mice; essentially no difference in ultimate strain was found between the genotypes. This is in contrast to the dramatic reduction in strain (−59%) and increased brittleness (+79%) in the mineralized bone of the *oim/oim* mice compared with the +/+ mice. Thus, the brittleness

of the *oim/oim* bone appears to be largely related to the mineral phase, and most likely to the abnormal interaction of the mineral phase with the collagenous matrix phase.

The fact that no differences exist between the ultimate strain of the demineralized matrices for the two genotypes was an unexpected result, given that an earlier study found substantial differences in strain-to-failure in tensile tests of tail tendons from these two genotypes [31], and another study found reduced stiffness in aortic collagen from these mice [32]. However, a recent study on SMAD6 mice by Silva et al. [33] found results similar to our studies. SMAD6 mice have disorganized collagen as well as reduced collagen content. Mechanical properties of mineralized SMAD6 bones revealed reduced post-yield displacement compared with controls, which the authors attribute in part to reduced collagen content. In spite of this, similar to our studies, tensile tests of demineralized femora from SMAD6 mice revealed no differences in ultimate strain compared with controls, but did find a 23% reduction in ultimate stress. Thus, in that study as well as in the current study, abnormal collagen content and organization affected displacement only in the mineralized bone, and not in the demineralized bone.

In contrast, the tensile tests performed by Misof et al. [31] on *oim/oim* mouse tail tendons revealed substantial differences in ultimate strain and stress relative to +/+ tendons, indicative of two very different materials. We have demonstrated in previous studies that, compared with +/+, collagen crosslinks are reduced in *oim/oim* bone and tendon [34], but it is very likely that the effect of this difference is more pronounced in tendon, whose composition is almost exclusively a linear arrangement of tightly bundled collagen fibrils. In demineralized bone matrix, the collagen fibrils presumably still reside in the same arrangement as that of mineralized bone, i.e., in lamellae whose collagen orientation varies to maximize its strength. In addition, however, non-collagenous proteins are still bonded to the collagen molecules and are present within the demineralized bone matrix, and may in fact stabilize the collagen fibrils so that the matrix structure is competent to withstand normal stresses. Thus, tensile testing of the entire demineralized bone matrix and all its components is likely to result in a different outcome compared with tensile testing of a predominantly collagenous structure such as tendon.

Bone integrity is dependent on both a mineral phase, biological apatite, and an organic matrix phase, primarily type I collagen, which interact to produce a composite material of distinct mechanical properties. Although it has been generalized that elasticity (stiffness) is related to the mineral phase and plasticity (ductility, toughness) to the organic matrix [35,36], the interaction of these two phase is critical. Though the material properties of *oim/oim* demineralized bone are not different from those of demineralized +/+ bone, *oim/oim* mineralized bone with a mechanically competent organic matrix displays greatly reduced plasticity. In fact, the post-yield region of the *oim/oim* bone was reduced by approximately 81% compared with the +/+ bones [22], translating into a greatly diminished capacity to absorb energy and prolong catastrophic failure. Thus, plasticity cannot solely be attributed to the organic matrix. A more likely explanation is that both the mineral and matrix phases are intimately involved, with the altered collagen template inhibiting the formation of a mechanically reliable bone composite. This unusual interaction between the two phases is manifested in changes in mineral:matrix ratio (mineralization density) [17,37], orientation and size of the mineral crystals [17–19], and bonding between mineral crystals and organic matrix in the *oim/oim* model [37], all of which may contribute to diminished biomechanical properties.

Attempts have also been made to understand the phenomenon of brittleness at the microstructural level. By comparing fracture surfaces in the Mov13 mouse with those in +/+ mice, the brittleness of the Mov13 bones was attributed largely to a loss of energy-dissipating features in the microstructure, such as lamellar interfaces [38]. The lamellar bone present in the Mov13 bone did not dissipate energy through interlamellar cleavage as did the +/+ bone

during fracture. In addition, the number of lamellar interfaces was decreased in the Mov13 mice compared with controls due to an 80% increase in woven bone tissue. In the *oim/oim* mouse, a study utilizing ultrasound critical-angle reflectometry also found evidence of increased woven bone content [39], suggestive of a related mechanism for increased brittleness. Notwithstanding these results, a high mineralization density, as in *oim/oim* mouse bone, would also very likely contribute to brittleness. Earlier studies by Currey have demonstrated this phenomenon very clearly [40,41], with the explanation that in a highly mineralized structure, insufficient mineral-collagen bonds exist to dissipate fracture energy, and the various crack-stopping mechanisms that can act when mineral crystals in bone have not coalesced are rendered ineffective when the volume fraction of mineral becomes too high.

Reduced crystallinity (size and perfection) of the *oim/oim* mineral phase may also contribute to the increased brittleness by allowing for a loss of energy-dissipating structures [17–19]. Earlier reports have linked changes in crystal size with abnormal bone mechanical properties [42,43], suggesting that a non-contiguous mineral phase resulting from a lack of lateral and longitudinal crystal fusion may exist. Landis previously reported a model of inadequate mineral continuity as a result of the altered collagen template in *oim* tendon [19]. An FTIR study from our group also found evidence of an abnormal apatite-collagen interaction, based on peak shifts in the apatitic phosphate region of *oim/oim* bone compared with +/+ bone [37]. Both experimental [44,45] and theoretical [46] studies have suggested that a change in the bonding between the mineral crystals and organic matrix plays an important role in bone tissue mechanics.

Finally, the role of collagen crosslinking in *oim/oim* bone fragility has not been fully explored. Prior work by our group and collaborators [34] revealed a 27% decrease in the level of the hydroxylysino-keto-norleucine (HLKNL) crosslinks in the *oim/oim* mouse bone and a 31% reduction in histidino-hydroxymerodesmosine (HHMD) crosslinks in tendon. We hypothesized that these crosslinks cannot form due to loose packing of the collagen molecules, i.e., increased water content of the fiber, rather than a distortion of the molecular structure [47]. Crosslinks are known to be crucial contributors to the mechanics of collagen, but the correlation between crosslinking and biomechanical properties of murine bone has not been elucidated precisely. Our results suggest that this reduction in crosslinks may be evidence of abnormal fiber packing, which alone does not substantially alter the bone matrix properties but does contribute to the alteration of the arrangement and crystallinity of the deposited bone mineral.

We are aware of some limitations to this study, most notably that mechanical tests on demineralized tissues can result in large standard deviations in the measured parameters, making it difficult to demonstrate significant differences between groups. Standard deviations as high as 46% in the +/+ strain values and 49% in the *oim/oim* stress values were found. Interestingly, large standard deviations such as these are not uncommon in tensile tests of demineralized bone. Wang et al. [48] reported standard deviations as high as 44% in both stress and strain measurements of their demineralized human bone samples, and Catanese et al [49] reported standard deviations as high as 67% in stress values obtained from tensile-tested demineralized bone. In the latter study, the authors concluded that monotonic mechanical properties of demineralized human and bovine bone can display substantial heterogeneity. The same may be true for the samples tested in the current study, where the process of demineralization could lead to inhomogeneities or larger variations in the demineralized group in comparison with the group of intact mineralized samples. If this is indeed true, it is possible that small, but real, differences in the material properties of the *oim/oim* and +/+ demineralized bone might exist, for example the 25% reduction in ultimate stress, but did not reach significance due to inadequate sample size. However, it is unlikely that differences as large as those between mineralized *oim/oim* and +/+ bone exist. Regardless of whether small, but

significant, differences are present or not, our overall conclusion remains the same: that the differences between the material properties of the mineralized +/+ and *oim/oim* bones are much greater than the differences between the properties of the demineralized bone matrix of these two genotypes.

Another factor to consider is the discrepancy that data from bend tests are being compared with data from tensile tests. In the tensile test, uniaxial tensile load is applied to the demineralized bone, and it can be assumed that the stress in the cross-section is uniformly distributed. Failure occurs at the weakest cross-section (the section with the smallest cross-sectional area in the case of uniform tensile stress) along the length of the bone, which in the mouse femur is near the midpoint. The bend tests performed on the mineralized bones were such that the maximum bending moment occurred in a similar central cross-section (the diaphyseal midpoint) as the maximum stress in the tensile test. Further, in three-point bending, bone experiences tensile stresses on one side of the bone and compressive stresses on the other side. Although shear forces may also be present, a recent study found the errors in elastic modulus for mouse femurs were on the order of 12–35%, dependent on mouse strain, which could be considered reasonable when compared with estimates based on other types of measurements [50]. Since bone is weaker in tension than in compression [51], it is also reasonable to assume that failure occurred on the tensile side.

In summary, the mechanism underlying the tissue fragility associated with OI may be more complex than previously recognized. The attribution of reduced bone plasticity, i.e., brittleness, to changes in the matrix phase alone is insufficient to explain the magnitude of bone fragility in the *oim/oim* mice. The results of this study support the concept that deficient material properties of the bone matrix itself are not the primary cause of bone fragility in this model of OI. Instead, the abnormal collagen scaffold serves as a template for abnormal mineral deposition, resulting in an incompetent mineral-matrix interaction that contributes significantly to the inferior material properties of the bone. Overall, the homotrimer collagen-based bone matrix is an important, but not the sole, contributor to fragility in *oim/oim* bone. Incorporating this into our current understanding of OI, we anticipate that greater insights into the mechanism of fragility in the *oim/oim* mice may ultimately lead to improved therapeutics in the clinical sphere.

Acknowledgments

This study was supported by NIH DE11803 and AR48337 (NPC), and utilized the facilities of the Core Center for Skeletal Integrity NIH AR46121.

References

1. Rowe, DS, Jr. Osteogenesis imperfecta. In: Avioli, LK.; Krane, SM., editors. Metabolic bone disease and clinically related disorders. San Diego: Academic Press; 1998.
2. Bachinger HP, Morris NP, Davis JM. Thermal stability and folding of the collagen triple helix and the effects of mutations in osteogenesis imperfecta on the triple helix of type I collagen. Am J Med Genet 1993;45:152–162. [PubMed: 8456797]
3. Bella J, Eaton M, Brodsky B, Berman HM. Crystal and molecular structure of a collagen-like peptide at 1.9 Å resolution. Science 1994;266:75–81. [PubMed: 7695699]
4. Mietz H, Kasner L, Green WR. Histopathologic and electron-microscopic features of corneal and scleral collagen fibers in osteogenesis imperfecta type III. Graefes Arch Clin Exp Ophthalmol 1997;235:405–410. [PubMed: 9248835]
5. Raghunath M, Bruckner P, Steinmann B. Delayed triple helix formation of mutant collagen from patients with osteogenesis imperfecta. J Mol Biol 1994;236:940–949. [PubMed: 8114103]
6. Stoss H, Freisinger P. Collagen fibrils of osteoid in osteogenesis imperfecta: Morphometrical analysis of the fibril diameter. Am J Med Genet 1993;45:257. [PubMed: 8456812]

7. Beck K, Chan VC, Shenoy N, Kirkpatrick A, Ramshaw JA, Brodsky B. Destabilization of osteogenesis imperfecta collagen-like model peptides correlates with the identity of the residue replacing glycine. Proc Natl Acad Sci USA 2000;97:4273–4278. [PubMed: 10725403]
8. Zionts LE, Nash JP, Rude R, Ross T, Stott NS. Bone mineral density in children with mild osteogenesis imperfecta. J Bone Joint Surg Br 1995;77:143–147. [PubMed: 7822373]
9. Boyde A, Travers R, Glorieux FH, Jones SJ. The mineralization density of iliac crest bone from children with osteogenesis imperfecta. Calcif Tissue Int 1999;64:185–190. [PubMed: 10024373]
10. Cepollaro C, Gonnelli S, Pondrelli C, Montagnani A, Martini S, Bruni D, Gennari C. Osteogenesis imperfecta: Bone turnover, bone density, and ultrasound parameters. Calcif Tissue Int 1999;65:129–132. [PubMed: 10430645]
11. Antoniazzi F, Bertoldo F, Mottes M, Valli M, Sirpresi S, Zamboni G, Valentini R, Tato L. Growth hormone treatment in osteogenesis imperfecta with quantitative defect of type I collagen synthesis. J Pediatr 1996;129:432–439. [PubMed: 8804334]
12. Rajtar M, Laszlo A, Beviz J, Bossanyi A, Almasi L, Csernay L. [Bone mineral content in osteogenesis imperfecta]. Orv Hetil 1996;137:1519–1523. [PubMed: 8757074]
13. Vetter U, Eanes ED, Kopp JB, Termine JD, Robey PG. Changes in apatite crystal size in bones of patients with osteogenesis imperfecta. Calcif Tissue Int 1991;49:248–250. [PubMed: 1760768]
14. Sarathchandra P, Kayser MV, Ali SY. Abnormal mineral composition of osteogenesis imperfecta bone as determined by electron probe X-ray microanalysis on conventional and cryosections. Calcif Tissue Int 1999;65:11–15. [PubMed: 10369727]
15. Chipman SD, Sweet HO, McBride DJ Jr, Davisson MT, Marks SC Jr, Shuldiner AR, Wenstrup RJ, Rowe DW, Shapiro JR. Defective pro alpha 2(I) collagen synthesis in a recessive mutation in mice: A model of human osteogenesis imperfecta. Proc Natl Acad Sci USA 1993;90:1701–1705. [PubMed: 8446583]
16. Phillips CL, Bradley DA, Schlotzhauer CL, Bergfeld M, Libreros-Minotta C, Gawenis LR, Morris JS, Clarke LL, Hillman LS. *Oim* mice exhibit altered femur and incisor mineral composition and decreased bone mineral density. Bone 2000;27:219–226. [PubMed: 10913914]
17. Camacho NP, Hou L, Toledano TR, Ilg WA, Brayton CF, Raggio CL, Root L, Boskey AL. The material basis for reduced mechanical properties in *oim* mice bones. J Bone Miner Res 1999;14:264–272. [PubMed: 9933481]
18. Fratzl P, Paris O, Klaushofer K, Landis WJ. Bone mineralization in an osteogenesis imperfecta mouse model studied by small-angle x-ray scattering. J Clin Invest 1996;97:396–402. [PubMed: 8567960]
19. Landis WJ. The strength of a calcified tissue depends in part on the molecular structure and organization of its constituent mineral crystals in their organic matrix. Bone 1995;16:533–544. [PubMed: 7654469]
20. McBride DJ Jr, Shapiro JR, Dunn MG. Bone geometry and strength measurements in aging mice with the *oim* mutation. Calcif Tissue Int 1998;62:172–176. [PubMed: 9437052]
21. McCarthy EA, Raggio CL, Hossack MD, Miller EA, Jain S, Boskey AL, Camacho NP. Alendronate treatment for infants with osteogenesis imperfecta: Demonstration of efficacy in a mouse model. Pediatr Res 2002;52:660–670. [PubMed: 12409511]
22. Misof BM, Roschger P, Baldini T, Raggio CL, Zraick V, Root L, Boskey AL, Klaushofer K, Fratzl P, Camacho NP. Differential effects of alendronate treatment on bone from growing osteogenesis imperfecta and wild-type mouse. Bone 2005;36:150–158. [PubMed: 15664013]
23. Camacho NP, Dow D, Toledano TR, Buckmeyer JK, Gertner JM, Brayton CF, Raggio CL, Root L, Boskey AL. Identification of the *oim* mutation by dye terminator chemistry combined with automated direct DNA sequencing. J Orthop Res 1998;16:38–42. [PubMed: 9565071]
24. Turner CH, Burr DB. Basic biomechanical measurements of bone: A tutorial. Bone 1993;14:595–608. [PubMed: 8274302]
25. Huang, AHRCL.; Fritton, JC.; Camacho, NP. Comparison of radiographic and micro CT-determined parameters in mouse bone specimens. 51st Orthopaedic Research Society Meeting; Washington, DC. 2005. p. 713
26. van der Meulen MC, Jepsen KJ, Mikic B. Understanding bone strength: Size isn't everything. Bone 2001;29:101–104. [PubMed: 11502469]

27. Jonas J, Burns J, Abel EW, Cresswell MJ, Strain JJ, Paterson CR. A technique for the tensile testing of demineralised bone. J Biomech 1993;26:271–276. [PubMed: 8468340]
28. Willis JB. Determination of calcium in blood serum by atomic absorption spectroscopy. Nature 1960;186:249–250. [PubMed: 13844983]
29. Shah KM, Goh JC, Karunanithy R, Low SL, Das De S, Bose K. Effect of decalcification on bone mineral content and bending strength of feline femur. Calcif Tissue Int 1995;56:78–82. [PubMed: 7796351]
30. Bradford MM. A rapid and sensitive method for the quantitation of microgram quantities of protein utilizing the principle of protein-dye binding. Anal Biochem 1976;72:248–254. [PubMed: 942051]
31. Misof K, Landis WJ, Klaushofer K, Fratzl P. Collagen from the osteogenesis imperfecta mouse model (*oim*) shows reduced resistance against tensile stress. J Clin Invest 1997;100:40–45. [PubMed: 9202055]
32. Pfeiffer BJ, Franklin CL, Hsieh FH, Bank RA, Phillips CL. Alpha 2(I) collagen deficient *oim* mice have altered biomechanical integrity, collagen content, and collagen crosslinking of their thoracic aorta. Matrix Biol 2005;24:451–458. [PubMed: 16095890]
33. Silva MJ, Brodt MD, Wopenka B, Thomopoulos S, Williams D, Wassen MH, Ko M, Kusano N, Bank RA. Decreased collagen organization and content are associated with reduced strength of demineralized and intact bone in the SAMP6 mouse. J Bone Miner Res 2006;21:78–88. [PubMed: 16355276]
34. Sims TJ, Miles CA, Bailey AJ, Camacho NP. Properties of collagen in OIM mouse tissues. Connect Tissue Res 2003;44 Suppl 1:202–205. [PubMed: 12952198]
35. Burstein AH, Zika JM, Heiple KG, Klein L. Contribution of collagen and mineral to the elastic-plastic properties of bone. J Bone Joint Surg Am 1975;57:956–961. [PubMed: 1184645]
36. Jepsen K, Mansoura MK, Kuhn JL, et al. An in vivo assessment of the contribution of type I collagen to the mechanical properties of cortical bone. Trans Orthop Res Soc 1992;17:93.
37. Camacho NP, Landis WJ, Boskey AL. Mineral changes in a mouse model of osteogenesis imperfecta detected by Fourier transform infrared microscopy. Connect Tissue Res 1996;35:259–265. [PubMed: 9084664]
38. Jepsen KJ, Goldstein SA, Kuhn JL, Schaffler MB, Bonadio J. Type-I collagen mutation compromises the post-yield behavior of Mov13 long bone. J Orthop Res 1996;14:493–499. [PubMed: 8676263]
39. Mehta SS, Antich PP, Landis WJ. Bone material elasticity in a murine model of osteogenesis imperfecta. Connect Tissue Res 1999;40:189–198. [PubMed: 10772540]
40. Currey JD. Effects of differences in mineralization on the mechanical properties of bone. Phil Trans R Soc Lond B Biol Sci 1984;304:509–518. [PubMed: 6142490]
41. Currey JD. The mechanical consequences of variation in the mineral content of bone. J Biomech 1969;2:1–11. [PubMed: 16335107]
42. Boskey AL, Gilder H, Neufeld E, Ecarot B, Glorieux FH. Phospholipid changes in the bones of the hypophosphatemic mouse. Bone 1991;12:345–351. [PubMed: 1782102]
43. Boskey AL, Rimnac CM, Bansal M, Federman M, Lian J, Boyan BD. Effect of short-term hypomagnesemia on the chemical and mechanical properties of rat bone. J Orthop Res 1992;10:774–783. [PubMed: 1403290]
44. Walsh WR, Guzelsu N. The role of ions and mineral-organic interfacial bonding on the compressive properties of cortical bone. Biomed Mater Eng 1993;3:75–84. [PubMed: 8369729]
45. Walsh WR, Guzelsu N. Compressive properties of cortical bone: mineral-organic interfacial bonding. Biomaterials 1994;15:137–145. [PubMed: 8011860]
46. Bundy KJ. Determination of mineral-organic bonding effectiveness in bone: Theoretical considerations. Ann Biomed Eng 1985;13:119–135. [PubMed: 4003875]
47. Miles CA, Sims TJ, Camacho NP, Bailey AJ. The role of the alpha2 chain in the stabilization of the collagen type I heterotrimer: A study of the type I homotrimer in *oim* mouse tissues. J Mol Biol 2002;321:797–805. [PubMed: 12206762]
48. Wang X, Li X, Bank RA, Agrawal CM. Effects of collagen unwinding and cleavage on the mechanical integrity of the collagen network in bone. Calcif Tissue Int 2002;71:186–192. [PubMed: 12200651]

49. Catanese J 3rd, Iverson EP, Ng RK, Keaveny TM. Heterogeneity of the mechanical properties of demineralized bone. J Biomech 1999;32:1365–1369. [PubMed: 10569717]

50. Schriefer JL, Robling AG, Warden SJ, Fournier AJ, Mason JJ, Turner CH. A comparison of mechanical properties derived from multiple skeletal sites in mice. J Biomech 2005;38:467–475. [PubMed: 15652544]

51. Reilly DT, Burstein AH. The elastic and ultimate properties of compact bone tissue. J Biomech 1975;8:393–405. [PubMed: 1206042]

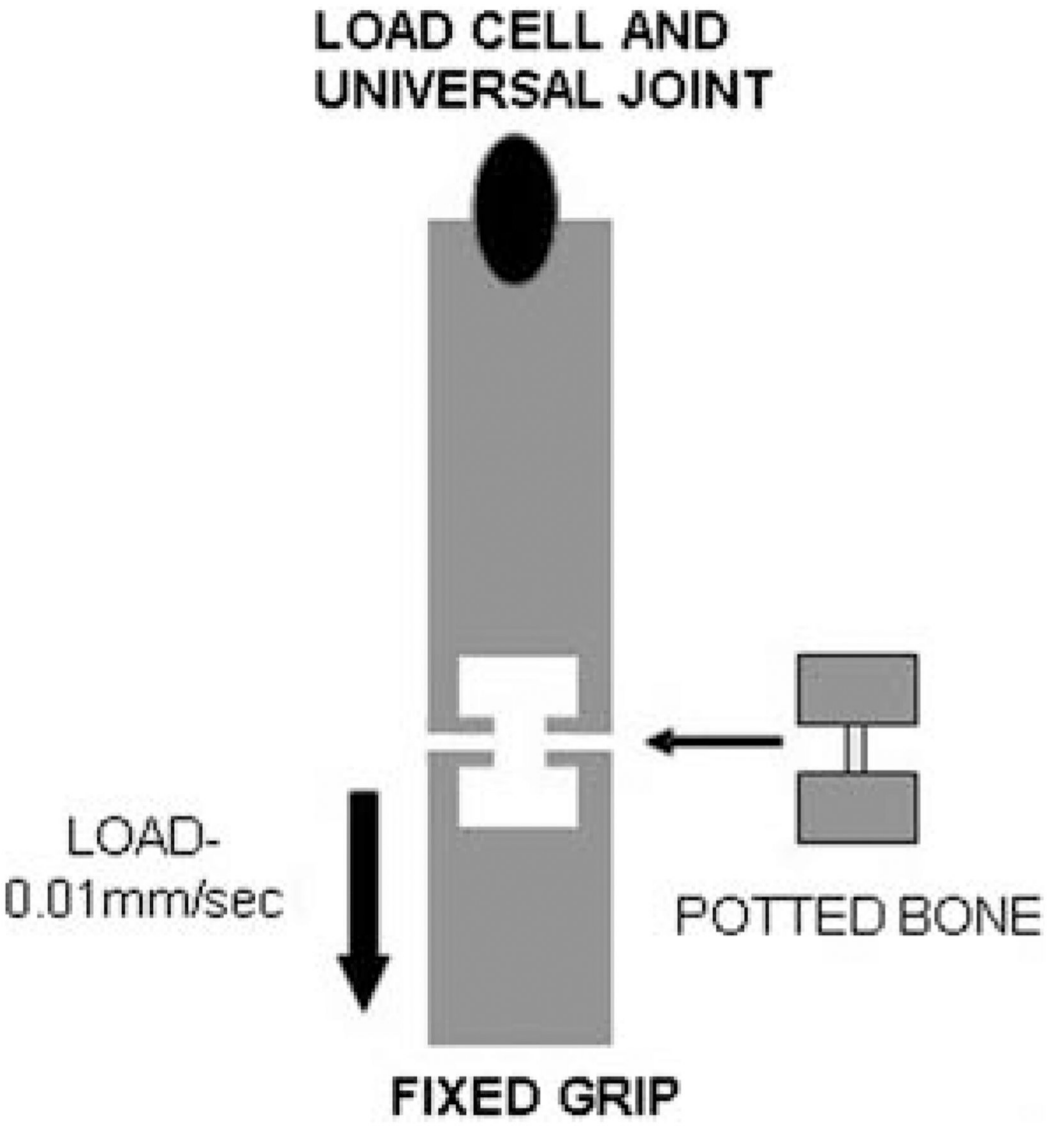

Fig. 1.
Schematic of tensile testing apparatus. The potted, demineralized femur was loaded under displacement control at a rate of 0.01 mm/sec until failure. The upper grip allowed free rotation, and the lower grip was fixed with respect to rotational movement

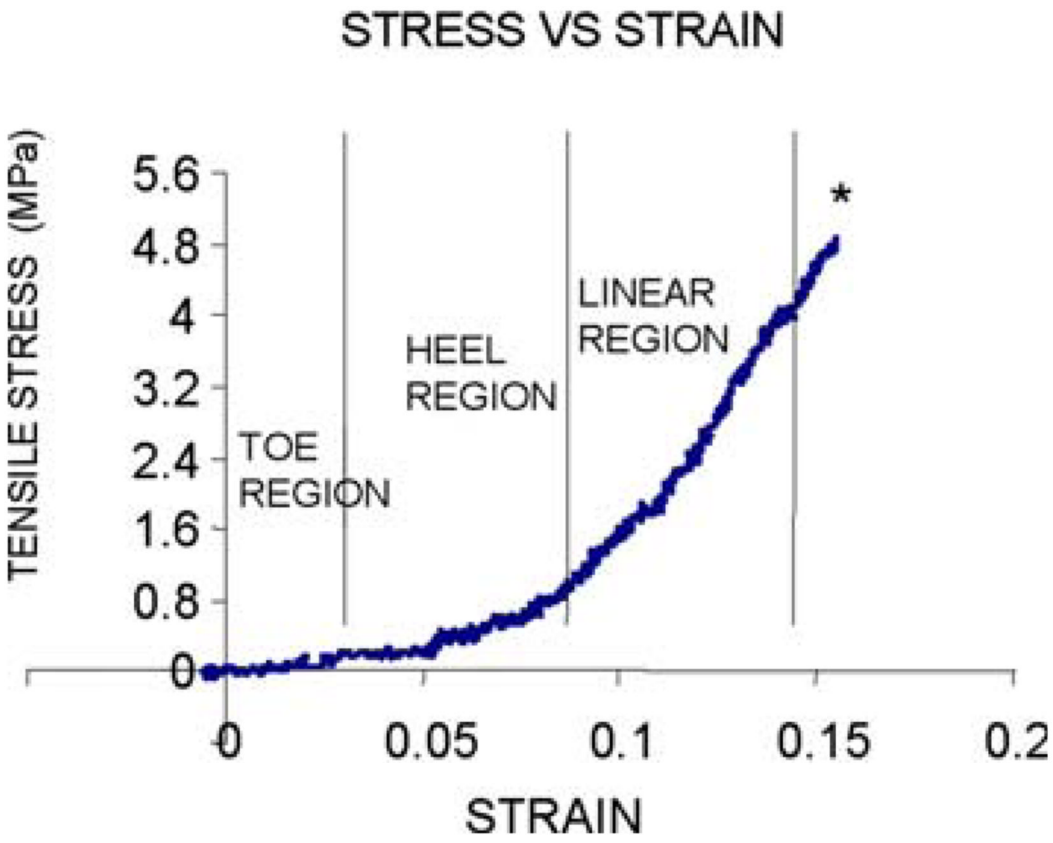

Fig. 2.

Representative tensile stress versus strain curve depicting toe, heel, and linear regions. The asterisk indicates the point of failure, which for each demineralized bone occurred upon fracture

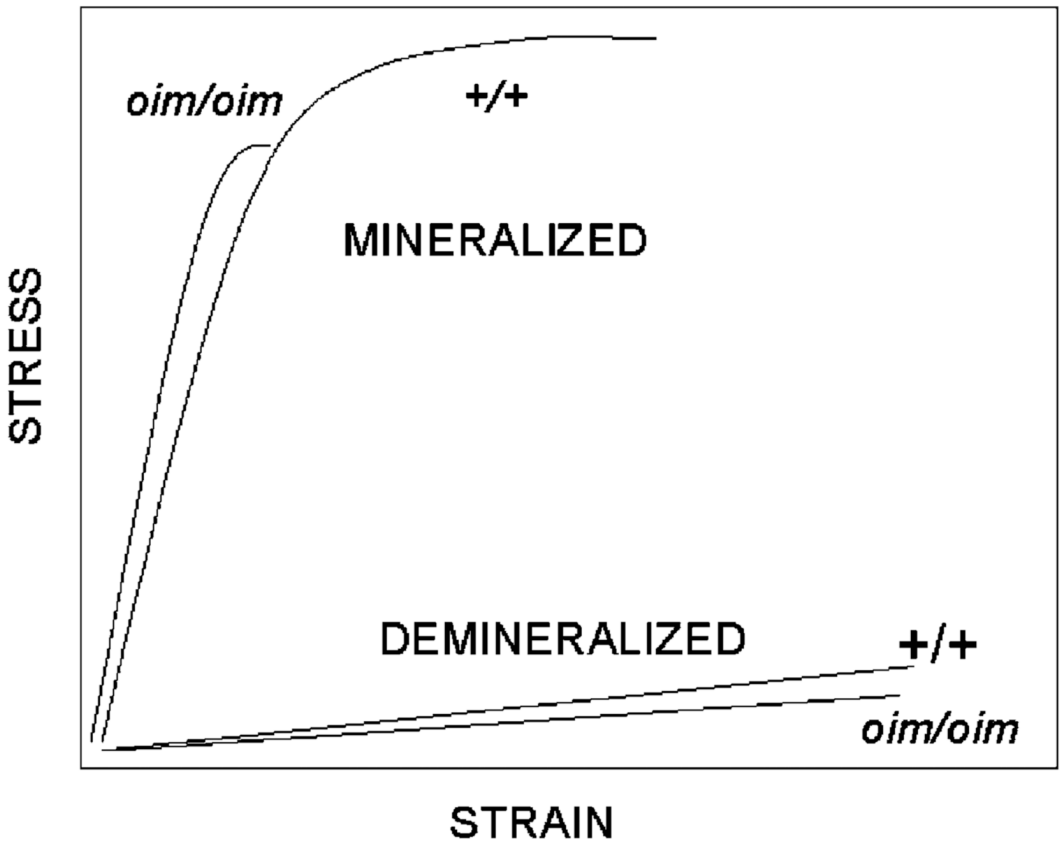

Fig. 3.
Schematic of mineralized and demineralized stress versus strain curves for wildtype (+/+) and *oim/oim* femora. Ultimate strain for the mineralized *oim/oim* bone is less than half that of the mineralized +/+ bone, while in the demineralized bones the values for the two genotypes are essentially equivalent

Table 1

Structural properties of femora from three-point bend tests

	+/+	*oim/oim*	% difference in *oim/oim* compared with +/+
n	14	15	
Load (N)	12.3 ± 1.53	6.13 ± 1.27*	−50.3
Deflection (mm)	0.73 ± 0.21*	0.32 ± 0.068*	−56.2
Stiffness (N/mm)	26.7 ± 5.14	17.8 ± 3.19*	−33.2
Work (N*mm)	5.58 ± 2.72	1.21 ± 0.43*	−78.3

Values are the mean ± SD

* $p < 0.05$ versus +/+

Table 2

Material properties of femora derived from three-point bend tests

	+/+	*oim/oim*	% difference in *oim/oim* compared with +/+
n	14	15	
Ultimate stress (MPa)	89.7 ± 13.9	77.1 ± 16.9*	−14.0
Ultimate strain	0.088 ± 0.027	0.036 ± 0.009*	−59.1
Young's modulus (GPa)	1.69 ± 0.44	2.44 ± 0.66*	+44.4
Toughness (N/m^2)	4.83 ± 1.37	1.49 ± 0.56*	−69.2
Brittleness (%)	51.1 ± 11.9	91.3 ± 14.8*	+78.7

Values are the mean ± SD

* $p < 0.05$ versus +/+

Table 3

Material properties of demineralized femora derived from tensile tests

	+/+	*oim/oim*	% difference in *oim/oim* compared with +/+
n	17	12	
Ultimate stress (MPa)	7.19 ± 2.51	5.42 ± 2.68*	−24.6
Ultimate strain	0.13 ± 0.06	0.12 ± 0.05	−7.7
Young's modulus (MPa)	18.9 ± 11.1	15.9 ± 8.1	−15.9
Toughness (N/m^2)	0.12 ± 0.05	0.09 ± 0.06	−25.0

Values are the mean ± SD

* $p = 0.09$ versus +/+